

Effect of Core Material on Breaking Behavior of Self-Bursting Microcapsules

Naoki Tsuda^{1,2}, Toshiro Ohtsubo¹, Masayoshi Fuji²

¹Health & Crop Sciences Research Laboratory, Sumitomo Chemical Co., Ltd., Takatsukasa, Takarazuka, Hyogo, Japan

²Ceramics Research Laboratory, Nagoya Institute of Technology, Honmachi, Tajimi, Gifu, Japan

E-mail: {tsudan, ootsubo}@sc.sumitomo-chem.co.jp, fuji@nitech.ac.jp

Received October 28, 2011; revised November 25, 2011; accepted December 8, 2011

Abstract

Self-bursting microcapsules, which retain their shape when suspended in water but burst quickly after the water evaporates, were proposed in a previous report. In this report, the effect of core materials on the bursting mechanism was studied. Five kinds of solvents were used as core materials, microencapsulated with polyurethane via an interfacial polymerization method. It was found that the self-bursting ratio was proportional to the measured dielectric constant of the core material. Thus, the solvents with a higher dielectric constant had an effect on the wall material to a greater extent. Furthermore, the self-bursting ratio was able to be predicted using the “organic conceptual diagram”.

Keywords: Microcapsule, Interfacial Polymerization, Self-Bursting, Dielectric Constant

1. Introduction

Microcapsules (MCs) are small containers whose wall material is mainly comprised of natural polymers, synthetic polymers, or inorganic compounds [1,2]. For this reason, MCs offer a number of interesting advantages to the cores they encapsulate including their protection, shelf life-enhancement, and controlled release. Thus, several researchers are actively investigating the applications of MC formulations in the pharmaceutical, printing, agricultural, and food industries [3-10]. Furthermore, numerous methods have been developed for preparing MCs, such as interfacial polymerization [3-5], in situ polymerization [7,8], coacervation [9], and spray-drying [10].

In a previous study [11], we reported a “breaking-type” MC that is destroyed upon application of an external force. “Breaking type” MC has been generally used in the field of pest control [11] because of the concept of the MC which is an example of a “long-duration release” profile. In contrast, a quick-release MC is demanded in certain areas of agriculture. For example, when a farmer sprays pesticide, the active ingredient (AIs) is preferably encapsulated by a material for safe handling. However, when applying the pesticide to a target, the capsule material becomes a hindrance for quick efficacy.

Previous reports on quick-release MCs [12-15] describe complicated synthesis techniques that are not often

commercially feasible, especially in the field of crop protection. Therefore, we focused on the established method of interfacial polymerization in order to prepare quick-release MCs [16].

In this study, we investigated the effect of the core material on the self-bursting phenomenon in MCs prepared via interfacial polymerization. Using five kinds of solvents for the core materials, we found that the dielectric constant of the core material was related to the self-bursting phenomenon. Furthermore, solvents with a higher dielectric constant had an effect on the wall material to a greater extent. Finally, self-burst ratio was able to be predicted using the organic conceptual diagram.

2. Materials and Methods

2.1. Materials

Pyriproxyfen was supplied by Sumitomo Chemical Co., Ltd. Nisseki Hisol SAS 296[®] (phenyl xylyl ethane (PXE)) was purchased from Nippon Oil Corporation. Methyl naphthalene (MNP), toluene, and ethyle acetate were purchased from Wako Pure Chemical Industries, Ltd[?]. Vincyzer 40[®] (Diisobutyl adipate (DIBA)) was obtained from Kao Corporation. Sumidur N-3300[®] (hexamethylene diisocyanate isocyanurate) was supplied by Sumika Bayer Urethane Co., Ltd. Ethylene glycol (EG) was obtained from

Showa Denko K. K., and gum arabic was purchased from San-ei Yakuhin Boeki Co., Ltd.

2.2. Preparation of Microcapsules

Five types of MCs with polyurethane walls, samples 1 - 5 in **Table 1**, were prepared by an interfacial polymerization method based on the previous report [16].

2.3. Characterization of Microcapsules

2.3.1. Reaction Rate of Isocyanate (NCO) Group [16]

2 g of the MC suspension were added to a 40 mL methanol solution and mixed with water at a volume ratio of 95/5 (v/v). The residual NCO group in Sumidur N-3300 was analyzed by high-performance liquid chromatography on a Zorbax CN column (5 μ m; 4.6 mm ϕ \times 25 cm). A UV absorption photometer was used as the detector (wavelength: 254 nm). The column temperature was 40°C.

2.3.2. Infrared Spectroscopy of Wall Material

30 g of each MC suspension were centrifuged. Then, the precipitated MC particles were first washed several times with deionized water by decantation. The samples were washed 3 times with acetone, next, washed 3 times with methanol and then dried in a vacuum for 24 h. The infrared spectrum of the obtained polymer was measured at room temperature with a Spectrum One (PerkinElmer Inc.) using the ATR method.

2.3.3. MC Observation

MCs were observed with a digital microscope (HI-SCOPE Advanced KH-3000, Hirox Co. Ltd.) at room temperature.

Table 1. Recipes for preparing MC particles by interfacial polymerization^a.

Ingredients / Sample No.	1	2	3	4	5
Pyriproxyfen ^b (g)	60.0	60.0	60.0	60.0	60.0
PXE (g)	60.0				
DIBA (g)	30.0	90.0			
MNP			90.0		
Toluene				90.0	
Ethyl acetate					90.0
Sumidur N-3300 (g)	0.72	0.72	0.69	0.76	0.74
Gum Arabic 8 wt% aqueous solution (g)	150.	150.	150.	150.	150.
Ethylene glycol (g)	7	7	7	7	7
	0.12	0.12	0.11	0.12	0.12

^aReaction temperature, 75°C; Reaction time, 48 h; ^bPurity, 99%.

2.3.4. Pyriproxyfen Content [16]

The pyriproxyfen concentration (C_0) in the MC suspension was determined by gas chromatography on a DB-1 column (0.25 mm ϕ \times 30 m) using Helium as the carrier gas. The average linear velocity was 30 cm/s, while the oven temperature was 230°C. The injection port and detector temperatures were both 250°C.

2.3.5. Entrapment Ratio [16]

First, water which was saturated with sodium chloride was prepared. Next, 5 g of the prepared MC suspensions were mixed with 15 mL of the sodium chloride solution. Then, 5 mL of decane was added and the dispersion was shaken at 300 times/min for 3 min to dissolve the AI outside the MC with decane. Subsequently, the dispersion was centrifuged at 3000 rpm for 5 min. The upper layer of decane solution, which included pyriproxyfen outside the MC (C_{out_0}), was analyzed by gas chromatography as described above in 2.3.4. The entrapment ratio was then calculated using the following equation.

$$\text{Entrapment ratio} = [(C_0 - C_{out_0})/C_0] \times 100 \quad (1)$$

2.3.6. Self-Burst Ratio [16]

A MC suspension (0.5 g) was diluted in 999.5 g of water. 5 grams of the diluted suspension were added to a Petri dish and allowed to dry naturally. After drying, 5 grams of decane were added to the Petri dish in order to rinse the dried MCs. Subsequently, the amount of pyriproxyfen outside the MC (C_{out_1}) in the decane solution was measured, as described above in 2.3.4. The self-burst ratio was then calculated using the following Equation.

$$\text{Self-burst ratio (\%)} = [(C_{out_1} - C_{out_0})/C_0] \times 100 \quad (2)$$

2.3.7. Measurement of Particle Size

The volume median diameter (D_{50}) and the particle distribution were measured using a particle size analyzer with laser diffraction system (Mastersizer 2000[®], Malvern Instruments Ltd.) at room temperature. The refractive index was 1.5.

2.3.8. Calculation of Wall Thickness

The wall thickness T was calculated using the following Equation [11].

$$T = (W_w/W_c)(r_c/r_w)(D/6) \quad (3)$$

where W_w is the weight of the wall material; W_c , the weight of the core material; ρ_w , the density of the wall material; and ρ_c , the density of the core material. The density of the wall material was measured using a pycnometer (Auto Pycnometer 1320, Shimadzu).

2.3.9. Measurement of Dielectric Constant

The dielectric constant of each solvent was measured using a 4284A precision LCR meter (Agilent Technologies, Inc). Measurement frequency range, measurement temperature, and electrode separation were 100 Hz-1 MHz, 25°C, and 0.3 mm, respectively.

2.3.10. Measurement of Glass Transition

Temperature (T_g)

5 g of the obtained MC suspension was freeze-dried for 24 h in order to evaporate the water using freeze dehydration equipment (FDU-540[®], TOKYO RIKAKIKAI CO. Ltd.). The obtained samples were washed with ethanol 3 times. Subsequently, the samples also were washed with acetone 3 times. The T_g of the MC wall was measured in an aluminum pan using differential scanning calorimetry (DSCQ100, TA instruments). The temperature was changed from -90°C to 50°C at the rate of 10°C/min under a nitrogen atmosphere.

3. Results and Discussion

The dielectric constant for each solvent is listed in **Table 2**. A higher dielectric constant indicates a higher polar character for the solvent. MNP and toluene, whose structures contain a benzene ring, exhibited a lower polarity than ethyl acetate and DIBA. The dielectric constant of mixture of PXE and DIBA was situated between the solvents which contained benzene structures and which contained esters.

First, relationship between rotation speed of homomixer and D₅₀ was examined using the recipes of **Table 1**. **Figure 1** shows D₅₀ as a function of rotation speed for the MCs with various solvents. D₅₀ varied with solvent type in the preparation, even though the rotation speed remained fixed. This result indicates that interfacial surface tension between the oil and water phases were different among the recipes shown in **Table 1**, which could be caused by the polar character of the solvent. As a result, it was found that D₅₀ was able to be controlled by rotation speed of homomixer and the solvent polarity had an

Table 2. Dielectric constant of solvents.

Solvents	Dielectric constant
Ethyl acetate	5.9
DIBA	4.8
PXE (10) + DIBA (5) [*]	3.4
MNP	2.6
Toluene	2.3

^{*}Mixture of PXE and DIBA in the weight ratio 10:5.

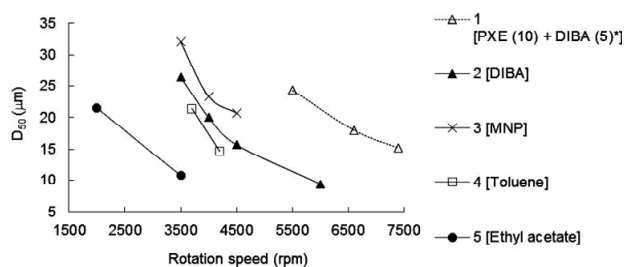


Figure 1. Relationship between rotation speed of homomixer (rpm) and D₅₀ (μm). The numbers and text in brackets show sample No. and solvent used in the core. ^{*}Mixture of PXE and DIBA in the weight ratio 10:5.

effect on D₅₀, thus the different rotation speeds in each recipe were needed for obtaining intended D₅₀.

In order to investigate the effect of core material on the self-burst phenomenon plainly, in the following discussion, D₅₀ was fixed for obtained MCs, which had almost the same particle size and T as shown in **Table 3**. **Figure 2** shows representative optical micrographs of the resulting MC particles, for DIBA, ethyl acetate. Except for MCs that used ethyl acetate, MC particles were spherical in shape, showed no aggregation, and had nearly the same values for D₅₀. Being highly soluble in water, ethyl acetate could have easily been dissolved in the water phase during the emulsification or polymerization steps and so the MC shape would change from spherical to that of a punctured balloon. A lot of coagulations were observed in the MCs sample used ethyl acetate. Hence, it was difficult to measure the particle size. As a result, it indicated that using highly polar solvent was not suitable for preparing “oil in water” type of MC.

Next, we confirmed the MC wall material if it was polyurethane. **Figure 3** shows the infrared spectrum of the wall materials of the MCs and the polymer prepared by mixing with Sumidur N-3300[®] and EG of which molar ratio of NCO group and OH group is 1:1. The polymerization was conducted at 75°C for 48 h.

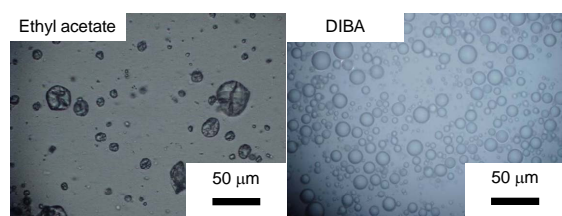
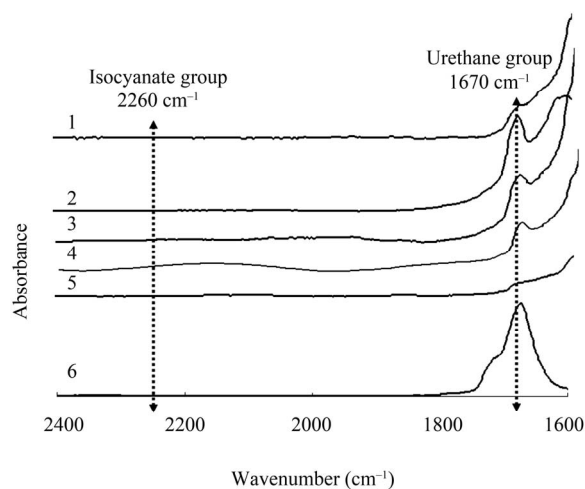
Sample No. and core solvent

- 1) Mixture of PXE and DIBA in the weight ratio 10:5
- 2) DIBA
- 3) MNP
- 4) Toluene
- 5) Ethyl acetate
- 6) Cast polymer made from Sumidur N3300 + EG

The specific absorption peak for the NCO groups at 2260 cm⁻¹ was disappeared, while that of the urethane groups around 1680 cm⁻¹ clearly appears [17]. All MC samples had the same spectrum, suggesting that polyurethane MCs were successfully obtained for all five core materials. In contrast, the intensity of urethane group peak using ethyl acetate was very low. It was presumed that firstly ethyl acetate partially dissolved into water

Table 3. Physico-chemical properties of the obtained MCs and the emulsification condition.

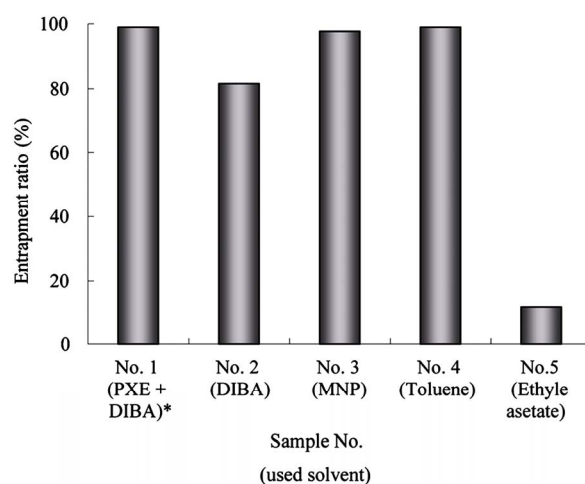
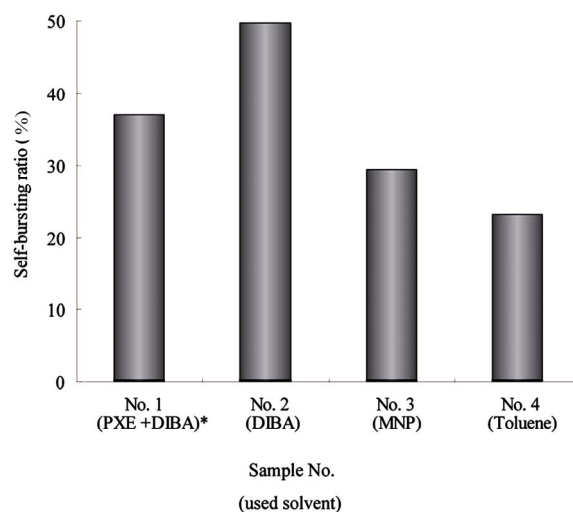
Properties / sample No.	1	2	3	4	5
Rotation speed (rpm)	6000	4300	4800	4300	2240
D (μm) [D ₁₀ /D ₅₀ /D ₉₀]	8.2/20.2/35.1	8.5/20.1/36.0	9.4/20.3/34.5	9.1/21.1/38.2	-
Calculated T (μm)	0.019	0.015	0.015	0.016	0.016
Pyriproxyfen content (%)	19.8	19.8	19.8	19.8	19.8
Reaction ratio of NCO group (%)	99	98	95	96	99

**Figure 2. Digital micrograph of MCs dispersed in water.****Figure 3. Infrared spectrum of wall materials.**

phase, and then a certain amount of Sumidur N3300 precipitated in the oil phase due to lack of the solvent to dissolve itself, thus effective amount of NCO group for the reaction was decreased. Additionally water also partially dissolved into ethyl acetate, subsequently the water reacted with NCO group, as a result, polyurethane group would be decreased.

The reaction rate of NCO group for all the samples were over 95% as shown **Table 3**. In this manner, we were able to successfully obtain MCs with uniform diameters. For all prepared MCs, the solvent and pyriproxyfen were encapsulated except for ethyl acetate as shown in **Figure 4**. The measured entrapment ratios support the micrograph observations presented in **Figure 2**.

In **Figure 5**, the measured self-burst ratio is shown for

**Figure 4. Entrapment ratio of pyriproxyfen in MCs. Relationship between core material and the entrapment ratio. Sample No. and the core material containing in the recipe are shown. *Mixture of PXE and DIBA in the weight ratio 10:5.****Figure 5. Self-burst ratio of MCs using different core solvents. Relationship between core material and the self-brust ratio. Recipe No. and the core material containing in the recipe are shown. *Mixture of PXE and DIBA in the weight ratio 10:5.**

each species. **Figure 6** shows the relationship between the self-burst ratio and the dielectric constant of the solvent. The self-burst ratio varied for each core solvent species and was proportional to the dielectric constant.

The relationship between self-burst ratio and dielectric constant may be caused by the changing crosslink density of the polyurethane wall with the core solvents. The mechanism was considered that the polymerization terminated at higher rate using high polarity solvent than using low one because the polar solvent attracted water and then, NCO group reacted with the water, as a result, amine group was produced. However, the amine group was not able to react with NCO group due to the lack of NCO groups as described above. Thus, the polymerization terminated at amine group, therefore crosslink density would be decreased.

Based on the assumption, we measured the glass transition temperature (T_g) of the wall materials instead of evaluating the crosslink density. **Figure 7** showed that the self-burst ratio increased with decreasing T_g . This relationship indicates that softer wall material which means low crosslink density is obtained with polar solvents.

Predicting the crosslink density of wall material is the first step towards controlling self-bursting in MCs. Whatever has been stated up to here, dielectric constant would become one of parameters for designing the wall material property. On the other hand, here, we focused on “Organic Conceptual Diagram”, which was easily calculable

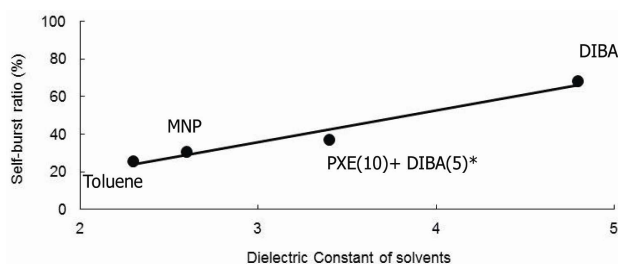


Figure 6. Relationship between dielectric constants and Self-burst ratio of MCs. *Mixture of PXE and DIBA in the weight ratio 10:5.

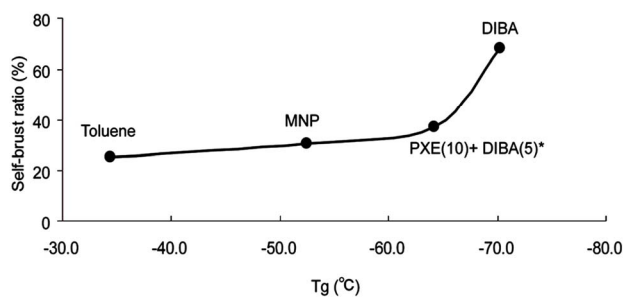


Figure 7. Relationship between T_g of wall materials and self-burst ratio. *Mixture of PXE and DIBA in the weight ratio 10:5.

Table 4. I/O value and the difference from the I/O value of polyurethane.

Materials	I/O value	Absolute value at difference in I/O value
Polyurethane	1.79	0
DIBA	0.42	1.36
PXE (10) + DIBA(5)*	2.56	0.77
MNP	10.66	8.87
Toluene	9.33	7.54

*Mixture of PXE and DIBA in the weight ratio 10:5.

parameter for representing polarity instead of dielectric constant, suggested by Fujita [18], as a way to determine compatibility between chemical materials [19]. We first investigated the compatibility between the wall material polymer and the core solvents. From their calculations, Oda *et al.* suggested that the ratio of inorganicity (I) to organicity (O) (I/O value) is one of the parameters that control compatibility [20]. **Table 4** shows the absolute I/O value of polyurethane and each solvent, along with the difference between the I/O value and that of polyurethane. According to these results, the I/O value of DIBA and a mixture of PXE/DIBA are more similar to that of polyurethane than MNP and toluene. These solvents also displayed higher self-bursting ratios as shown in **Figure 5**. In this sense, the “Organic Conceptual Diagram” would be used to indicate the compatibility between polymer and solvent for the design of self-bursting MCs. Specifically, solvents with an I/O value closest to the polyurethane MC wall material can be predicted to have higher self-bursting ratios.

4. Conclusions

The affect of core material to the self-bursting phenomenon was investigated. The dielectric constant of the solvent, a measure of polarity, showed a good correlation with the self-bursting ratio. The result suggested that crosslink density of the polyurethane wall was changed using higher polarity solvents compared to those with lower polarity. This idea was confirmed by observing that the wall material used polar solvent as the core material showed a lower glass transition temperature, indicating a less crosslink density. Finally, it was found that the “Organic Conceptual Diagram” would be used to predict compatibility between the polyurethane wall and the core solvents, resulting enable the design of the self-bursting ratio.

5. References

- [1] K. Miyata and Y. Nakahara, “The Preparation of Inor-

- ganic Particles by Interfacial Reaction,” *Progress in Organic Coatings*, Vol. 5, No. 2, 1977, pp. 115-129. [doi:10.1016/0300-9440\(77\)80006-4](https://doi.org/10.1016/0300-9440(77)80006-4)
- [2] G. Hadiko, H. Y. Sheng, M. Fuji and M. Takahashi, “Synthesis of Hollow Calcium Carbonate Particles by the Bubble Templating Method,” *Materials Letters*, Vol. 59, No. 29-30, 2005, pp. 2519-2522. [doi:10.1016/j.matlet.2005.03.036](https://doi.org/10.1016/j.matlet.2005.03.036)
- [3] J. Heidi and B. S. Ruth, “Preparation of Polyurethane Nanocapsules by Miniemulsion Polyaddition,” *Journal of Microencapsulation*, Vol. 24, 2007, pp. 731-742. [doi:10.1080/02652040701585179](https://doi.org/10.1080/02652040701585179)
- [4] N. Yan, P. Ni and M. Zhang, “Preparation and Properties of Polyurea Microcapsules with Non-Ionic Surfactant as Emulsifier,” *Journal of Microencapsulation*, Vol. 10, No. 3, 1993, pp. 375-383. [doi:10.3109/02652049309031527](https://doi.org/10.3109/02652049309031527)
- [5] H. B. Scher, “Microencapsulation of Pesticide by Interfacial Polymerization: Process and Performance Consideration,” *Pesticide Chemistry-Human Welfare and Environment*, Vol. 4, 1983, pp. 295-300.
- [6] M. Cakhshae, R. A. Pethrick, H. Rashid and D. C. Sherrington, “Encapsulation of carbon black in suspension polymerized copolymers,” *Polymer Communications*, Vol. 26, 1985, pp. 185-192.
- [7] H. Y. Lee, S. J. Lee, I. W. Cheong and J. H. Kim, “Microencapsulation of Fragrant Oil via *in Situ* Polymerization: Effects of pH and Melamine-Formaldehyde Molar Ratio,” *Journal of Microencapsulation*, Vol. 19, No. 5, 2002, pp. 559-569. [doi:10.1080/02652040210140472](https://doi.org/10.1080/02652040210140472)
- [8] H. Kage, H. Kawahara, N. Hamada, T. Kotaka and H. Ogura, “Operating Conditions and Microcapsules Generated by *in Situ* Polymerization,” *Advances in Powder Technology*, Vol. 13, No. 3, 2002, pp. 265-285. [doi:10.1163/156855202320252444](https://doi.org/10.1163/156855202320252444)
- [9] H. G. Bungenberg de Jong and H. R. Kruyt, “Colloid Science,” Elsevier, Amsterdam, 1949, pp. 232-258.
- [10] S. K. Ghosh, “Functional Coatings and Microencapsulation: A General Perspective,” In: S. K. Ghosh, Ed., *Functional Coatings: By Polymer Microencapsulation*, Wiley-VCH, Verlag GmbH & Co. KgaA, Weinheim, 2006, pp. 1-28.
- [11] T. Ohtsubo, S. Tsuda and K. Tsuji, “A Study of the Physical Strength of Fenitrothion Microcapsules,” *Polymer*, Vol. 32, No. 2, 1991, pp. 2395-2399. [doi:10.1016/0032-3861\(91\)90080-3](https://doi.org/10.1016/0032-3861(91)90080-3)
- [12] H. Shang-Hsiu, T. Chia-Hui, L. Chen-Fu, L. Dean-Mo and C. San-Yuan, “Controlled Rupture of Magnetic Polyelectrolyte Microcapsules for Drug Delivery,” *Langmuir*, Vol. 24, No. 20, 2008, pp. 11811-11818. [doi:10.1021/la801138e](https://doi.org/10.1021/la801138e)
- [13] G. Bruno, M. Michael, D. Jo, S. Stefaan and H. Wim, “Microcapsules Ejecting Nanosized Species into the Environment,” *J. A. C. S. Communications*, Vol. 130, 2008, pp. 14480-14482. [doi:10.1021/ja806574h](https://doi.org/10.1021/ja806574h)
- [14] B. Matthieu, G. Bruno, M. Helmuth, S. Gleb and S. Andre, “Direction Specific Release from Giant Microgel-Templated Polyelectrolyte Microcontainers,” *Soft Matter*, Vol. 5, 2009, pp. 3927-3931. [doi:10.1039/b909919k](https://doi.org/10.1039/b909919k)
- [15] L. Li, W. Wei, J. Xiao-Jie, X. Rui and C. Liang-Yin, “Smart Thermo-Triggered Squirting Capsules for Nanoparticle Delivery,” *Soft Matter*, Vol. 6, 2010, pp. 3759-3763. [doi:10.1039/c002231d](https://doi.org/10.1039/c002231d)
- [16] N. Tsuda and T. Ohtsubo, “Study on the Breaking Behavior of a Microcapsule,” *17th International Symposium on Microencapsulation*, Nagoya, September 2009, p. 7.
- [17] D. J. David and H. B. Staley, “Analytical Chemistry of the Polyurethanes,” Kreiger, Huntington, 1969, pp. 170-245.
- [18] A. Fujita, “Prediction of Organic Compounds by Conceptual Diagram,” *Chemical & Pharmaceutical Bulletin*, Vol. 2, No. 2, 1954, pp. 163-173.
- [19] K. Yoshio, S. Sato and Y. Honma, “Shinban Yukigaine-nezu kisotoouyo,” Sankyosyupan, 2008.
- [20] R. Oda, “Senryo kagaku,” Kyourituzensho, 1954.